Chemistry & Biology
Article

Dual Carbamoylations on the Polyketide and Glycosyl Moiety by Asm21 Result in Extended Ansamitocin Biosynthesis

Yan Li,[1,3] Peiji Zhao,[2,3] Qianjin Kang,[1] Juan Ma,[2] Linquan Bai,[1,*] and Zixin Deng[1]
[1]State Key Laboratory of Microbial Metabolism, School of Life Sciences and Biotechnology, Shanghai Jiao Tong University, Shanghai 200240, China
[2]State Key Laboratory of Phytochemistry and Plant Resources in West China, Kunming Institute of Botany, Chinese Academy of Sciences, Kunming, 650204, China
[3]These authors contributed equally to this work
*Correspondence: bailq@sjtu.edu.cn
DOI 10.1016/j.chembiol.2011.11.007

SUMMARY

Carbamoylation is one of the post-PKS modifications in ansamitocin biosynthesis. A novel ansamitocinoside with carbamoyl substitution at the C-4 hydroxyl group of the *N*-β-D-glucosyl moiety was identified from the ansamitocin producer, *Actinosynnema pretiosum*. Through biotransformation, the carbamoyltransferase gene *asm21* was suggested to be responsible for the carbamoylation of the glucosyl moiety. Three new derivatives without the backbone carbamoyl group were isolated from an *asm21* mutant and characterized by NMR spectroscopy. Among them, 18-*O*-methyl-19-chloroproansamitocin was the major product and the preferred substrate for macrolactam C-7 carbamoylation by Asm21. However, Asm21 exhibited higher catalytic efficiency toward the glucosyl moiety. Furthermore, the dual carbamoylations and *N*-glycosylation were precisely demonstrated in vivo. This work represents the first biochemical characterization of an *O*-carbamoyltransferase performing dual actions on both a polyketide backbone and a glycosyl moiety during ansamitocin biosynthesis.

INTRODUCTION

Carbamoylations are widespread in both primary and secondary metabolism, and mostly take place at heteroatoms such as oxygen or nitrogen. In antibiotic biosynthesis, although *N*-carbamoylation has been found in some cases, *O*-carbamoylation is relatively more common. It can be further divided into two types according to the positions modified: (1), the C-3 or C-4 hydroxyl group of hexose moieties, as in novobiocin and concanamycin A (Gellert et al., 1976; Haydock et al., 2005; Kinashi et al., 1984; Steffensky et al., 2000); or (2), a hydroxyl group of the nonsugar backbone, as in ansamitocins (**1**) and cephamycin C (Higashide et al., 1977; Miller et al., 1972; Nagarajan et al., 1971) (Figures 1A and 1B). The presence of the carbamoyl group is essential for antibiotic activity and cytotoxicity. An X-ray structure of the novobiocin-GyrB complex revealed interactions of the 3′-*O*-carbamoyl group with the amide nitrogen of Ala47, the side chain of Asp73, and also three ordered water molecules in the ATP binding site (Lewis et al., 1996). Removal of the carbamoyl group led to a dramatic decrease in inhibitory activity (Flatman et al., 2006; Hooper et al., 1982). The C-7/C-9 cyclic carbinolamide group of maytansinoids was proposed to act as an alkylating functionality involved in their antitumor activity. Blockage of ring opening of the carbinolamide by alkylation of the C-9 alcohol resulted in a marked decrease in antitumor activity and cytotoxicity (Kupchan et al., 1978).

Maytansinoids are potent antitumor agents that exert their cytotoxicity by disrupting microtubule assembly (Cassady et al., 2004). Antibody conjugates of maytansinoids exhibit increased tumor selectivity and longer circulation half-life and are in different stages of clinical development (Chari, 2008). Ansamitocins, produced by *Actinosynnema pretiosum* ssp. *auranticum* ATCC31565, are maytansinoids of microbial origin (Higashide et al., 1977). In the biosynthesis of ansamitocin P-3 (**1**), 3-amino-5-hydroxybenzoic acid (AHBA) is used as a starter unit (Floss et al., 2011), and the incorporation of seven PKS extender units gives a 19-membered macrolactam, proansamitocin (**9**), which further undergoes a series of post-PKS modifications, including *O*- and *N*-methylation, chlorination, epoxidation, *O*-carbamoylation, and *O*-acylation (Yu et al., 2002). Based on sequence homology, gene *asm21* in the biosynthetic gene cluster of ansamitocin was assigned the putative function of introducing the cyclic carbinolamide group. An *asm21*-inactivated mutant accumulated several compounds all lacking the carbamoyl group, indicating that *asm21* encodes a carbamoyltransferase (Spiteller et al., 2003).

Recently, ansamitocinosides P-1, P-2, and P-3 (AGP-1, AGP-2, and AGP-3, **2**) were isolated from *A. pretiosum* cultivated on solid yeast extract-malt extract-glucose (YMG) medium, which carry a β-D-glucosyl moiety attached to the amide nitrogen in place of the *N*-methyl group of ansamitocins (Lu et al., 2004; Ma et al., 2007; Zhao et al., 2008). Meanwhile, a series of polar ansacarbamitocins with a glucosyl moiety and three carbamoyl groups were isolated from *Amycolatopsis* sp. CP2808 (Snipes et al., 2007) (Figure 1C). Later on, Asm25 was proved to be the dedicated *N*-glycosyltransferase for the sugar attachment, representing the first enzymatically active antibiotic *N*-glycosyltransferase purified from inclusion bodies in *Escherichia coli* (Zhao et al., 2008). Moreover, two new

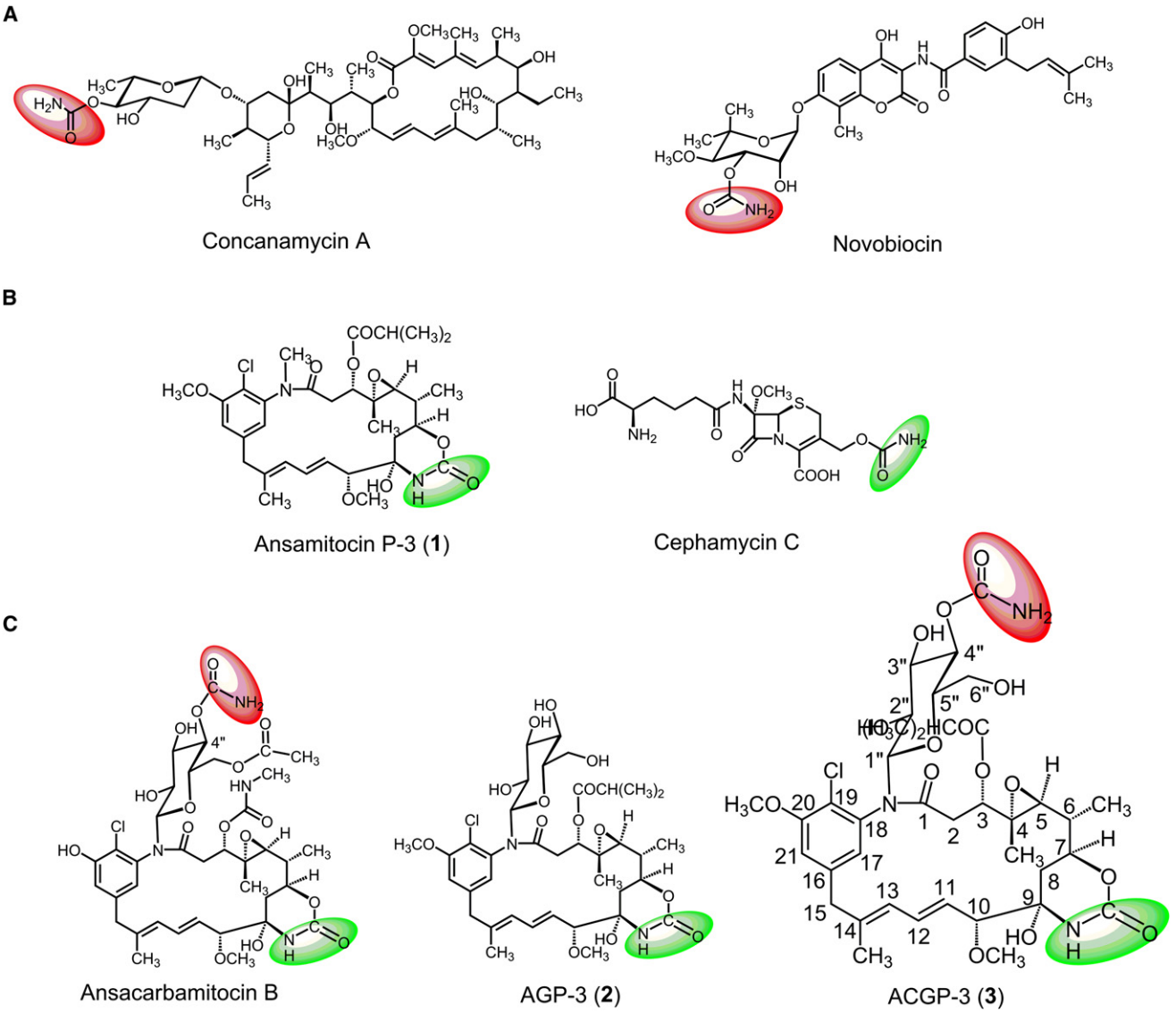

Figure 1. Two Types of Carbamoylation and Structure of 4″-*O*-Carbamoyl Ansamitocinoside P-3 (ACGP-3, 3)

(A) Antibiotics with carbamoylated sugar moieties.

(B) Antibiotics with carbamoylated nonsugar groups.

(C) AGP-3 (**2**), ACGP-3 (**3**), and ansacarbamitocin B. Carbamoyl groups on sugar moieties and nonsugar groups are highlighted in red and green, respectively. See also Table S2.

ansamitocin derivatives produced by mutational biosynthesis were assigned to be *N*-β-D-glucopyranosylated at the macrolactam amide (Knobloch et al., 2011).

Herein, we report the isolation of a naturally carbamoylated ansamitocinoside and the biochemical analysis of Asm21 action toward both the polyketide backbone and the ansamitocinoside sugar moiety.

RESULTS

Isolation and Structure Elucidation of 4″-*O*-Carbamoyl Ansamitocinoside P-3

By using an improved preparative TLC method (Ma et al., 2007), a novel carbamoyl ansamitocin *N*-glycoside (**3**, 12 mg) was obtained as a straw yellow powder from the ethyl acetate extract of *A. pretiosum* cultivated on solid YMG media (6 l). It was readily determined by NMR comparison with AGP-3 (**2**) to be an ansamycin of the ansamitocinoside-type (Table S2 available online). The ^{13}C-NMR and DEPT spectra of **3** showed 38 carbon signals including 7 methyl, 4 methylene, 16 methine, and 11 quaternary carbons, giving one more quaternary carbon signal (δ 159.3) in **3** than in **2**. The proton at δ 3.10 (H-4″) in **2** was shifted to δ 4.28 (H-4″) in **3**, indicating an acylation at the 4″-hydroxyl group (esterification effect). The molecular formula of **3** was determined to be $C_{38}H_{52}ClN_3O_{15}$ based on the quasi molecular ion peak at m/z 848.2988 $[M + Na]^+$ recorded by high resolution electrospray ionization mass spectrometry (HR-ESI-MS) in positive ion mode. Comparison of the molecular formula of **3** with that

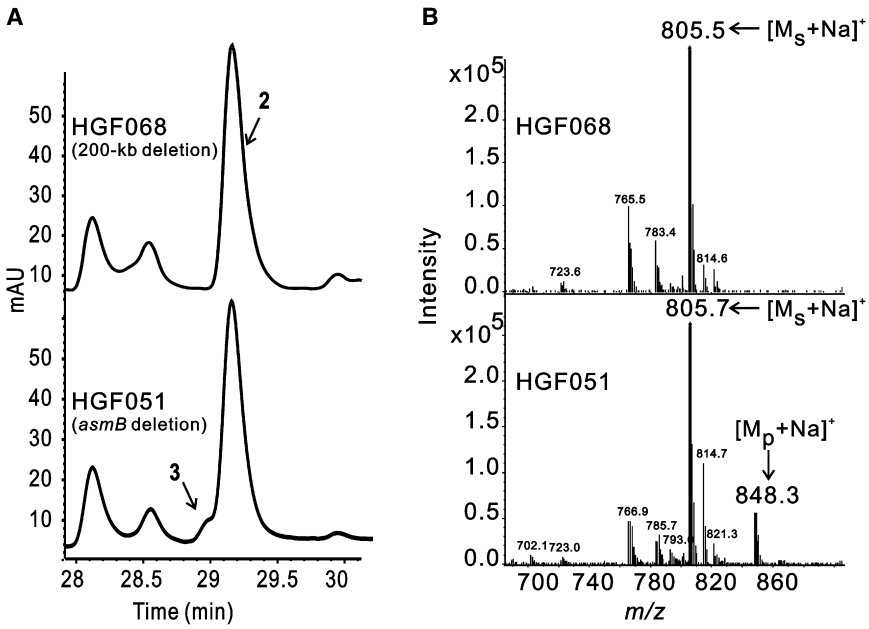

Figure 2. Carbamoylation of 2 through Feeding Experiments with Resting Cells

(A) HPLC analysis of the resting cell cultures of HGF068 and HGF051 fed with **2**.

(B) MS profiles of the resting cell cultures of HGF068 and HGF051 fed with **2**. M_s, Mw of **2**; M_p, Mw of **3**.

of **2** revealed the presence of a carbamoyl (-$CONH_2$) group in **3**. The position of this carbamoyl group was located at the 4-hydroxyl group of the β-D-glucopyranosyl moiety by ^1H-^{13}C long-range (HMBC) correlations between the proton at δ 4.28 (H-4″) and the carbons C-5″ (δ 78.5), C-6″ (δ 62.9), and $NH_2\underline{C}O$-4″ (δ 159.3), consistent with acylation at the 4″-hydroxyl group as indicated by the ^1H-NMR. Therefore, **3** was determined to be macrolactam amide *N*-desmethyl-*N*-β-D-[4-*O*-carbamoyl]-glucopyranosyl ansamitocin P-3 (ACGP-3) (Figure 1C).

Localization of Gene(s) for Carbamoylation of the C-4″ Hydroxyl Group in Ansamitocinoside P-3

The isolation of carbamoylated ansamitocin *N*-glycosides raised the question of what carbamoyltransferase(s) is(are) responsible for these carbamoylation reactions. Two mutants of *A. pretiosum*, HGF068 and HGF051, were used to discover the carbamoyltransferase gene responsible for the carbamoylation of **2**. The production of ansamitocins or any intermediates was totally abolished in both strains because of the absence of the PKS genes. The mutant HGF068 has a 200-kb deletion and lacks the whole *asm* gene cluster including *asm21*, whereas the mutant HGF051 carries a deletion of the PKS gene *asmB* but retains all the post-PKS modification genes (Yu et al., 2002) (Table S1). Feeding experiments with **2** in resting cell cultures of HGF051 or HGF068 were performed and the culture extracts were analyzed by LC-MS. Both the quasi molecular ion peaks of **2** ($[M + H]^+$ at m/z 783, $[M + Na]^+$ at m/z 805) and the expected quasi molecular ion peaks of **3** ($[M + H]^+$ at m/z 826, $[M + Na]^+$ at m/z 848) were detected in the HGF051 extract, whereas only **2** was found in the HGF068 extract (Figure 2). The results indicate that the gene(s) responsible for the carbamoylation of the glucosyl moiety is(are) located in the 200-kb region, and *asm21* is the most likely candidate.

Characterization of Four Compounds Isolated from the *asm21* Mutant

An *asm21*-disrupted mutant, named BLQ16, was constructed by the ReDirect technology (Gust et al., 2003) to obtain substrate for in vitro analysis of Asm21. A 1929-bp internal fragment of *asm21* was replaced with a 1384-bp disruption cassette containing *oriT* and the apramycin resistant gene *aac(3)IV* (Figure 3A). PCR validation was performed using genomic DNA of BLQ16 as template and asm21-det-F/R as primers. As expected, the amplified product of BLQ16 is 1.80 kb, whereas that of the wild-type is 2.30 kb (Figure 3B). LC-MS analysis showed that the production of ansamitocins was completely abolished in BLQ16. Furthermore, ansamitocin productivity in the mutant was partly restored by complementation with the cloned *asm21* gene under the control of the *PermE** promoter, confirming the involvement of *asm21* in ansamitocin biosynthesis (Figure 3C). In addition to the previously identified 19-chloroproansamitocin (**5**) (Spiteller et al., 2003), three novel compounds were isolated from the culture of BLQ16 on solid YMG medium and characterized by NMR (Figure 3D and Tables S3–S5). From 6 l of solid culture, ~60 mg 20-*O*-methyl-19-chloroproansamitocin (**8**), 5 mg 19-chloroproansamitocin (**5**), 5.5 mg 14-β-hydroxy-20-*O*-methyl-19-chloroisoproansamitocin (**6**), and 5.3 mg 14-α-hydroxy-20-*O*-methyl-19-chloroisoproansamitocin (**7**) were obtained (the configuration at C-14 of **6** and **7** may be interchanged). However, when BLQ16 was cultivated in liquid YMG medium, **5** was the major product with all other three components accumulated in lesser amounts as previously reported (Spiteller et al., 2003). Therefore, it is worth investigating whether **5** or **8** is the preferential substrate for Asm21.

Definition of Boundaries of *asm21*

For complementation of the *asm21*-disrupted mutant BLQ16, the open reading frame (ORF) previously (Yu et al., 2002) proposed for *asm21* based on alignments with known carbamoyltransferases, was amplified and expressed under the control of the strong constitutive *PermE** promoter in pJTU839 (Figure S1 and Table S1). However, pJTU839 failed to restore ansamitocin production. Re-analysis of the sequence using FramePlot 3.0 (Ishikawa and Hotta, 1999) revealed more potential start codons in the upstream sequences. Thus the longest ORF with an additional 198-bp in the 5′-region was chosen to ensure the integrity of this gene in the new plasmid pJTU3053 (Figure S1 and Table S1). As described above, complementation of BLQ16 with pJTU3053 restored ansamitocin production, indicating

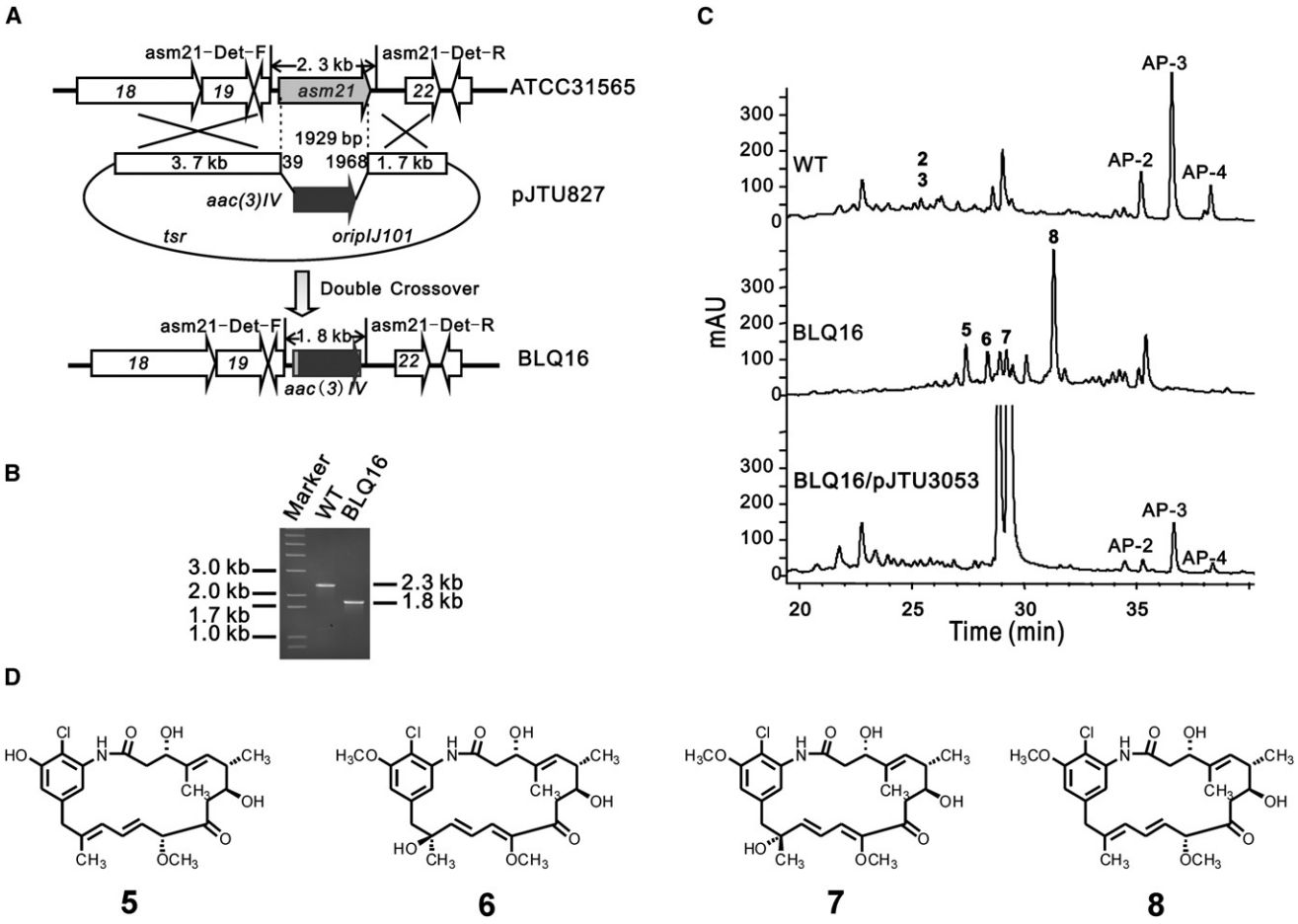

Figure 3. Inactivation and Complementation of *asm21*

(A) Schematic representation of *asm21* inactivation by ReDirect technology. A 1929-bp internal fragment of *asm21* was replaced by a 1384-bp disruption cassette containing *oriT* and the apramycin resistance gene *aac(3)IV*.

(B) PCR analysis of wild-type and mutant BLQ16. Using asm21-det-F/R as primers, the amplified product of BLQ16 was 1.80 kb, whereas that of the wild-type was 2.30 kb.

(C) HPLC analysis of the wild-type, mutant BLQ16, and BLQ16 complemented with *asm21* cloned under control of the *PermE** promoter. See also Figure S1.

(D) Chemical structures of four compounds isolated from BLQ16, the configuration of 6 and 7 at C-14 may be interchanged. See also Tables S3–S5.

that the N-terminal 66-aa segment or part of it is required for carbamoylation by Asm21.

Asm21 contains about 100 amino acids at its C terminus that are absent in the carbamoyltransferases involved in some other antibiotic biosynthesis. To probe whether this region of the protein was essential for catalytic activity and what its role might be, the 294-bp 3′ terminus of *asm21* was removed. However, complementation using two truncated versions of *asm21* failed to restore ansamitocin production (Figure S1). Significantly also, no accumulation of compounds with a linear carbamoyl side chain was observed. Thus, the C-terminal 97 amino acids of Asm21 are essential for the carbamoyl transferase activity of the protein.

Asm21 Catalyzes the Carbamoylation of the C-7 Hydroxyl Group on the Ansamitocin Backbone

The intact *asm21* fragment from pJTU3053 was cloned for expression. Asm21 was expressed in *E. coli* BLR(DE3)pLysE as an N-terminally His_6-tagged fusion protein in a yield of ~300 μg/l culture as determined by Bradford protein assay (Figure S2A). The calculated molecular weight of native and His6-tagged Asm21 is 80 kDa and 84 kDa, respectively. Based on the results with BLQ16, **8** was chosen to examine the enzymatic properties of Asm21 using carbamoyl phosphate as the second substrate in the presence of Mg^{2+} and ATP (Freel Meyers et al., 2004; Xu et al., 2004)., The reaction product was proven to be *N*-desmethyl-4,5-desepoxy-maytansinol (**4**) by LC-MS comparison with an authentic standard (Spiteller et al., 2003) (Figure 4A and Figure S2B).

The product of the enzymatic reaction was quantitated by HPLC with authentic **4** as an external standard. Based on the reaction temperature profile from 10°C to 50°C, purified Asm21 was optimally active at 37°C, assaying at a protein concentration of 1.6 μM in a 1 hr incubation. Comparable activities were exhibited between 30°C and 40°C and more than 40% of the maximal activity was retained above 50°C (Figure S3A).

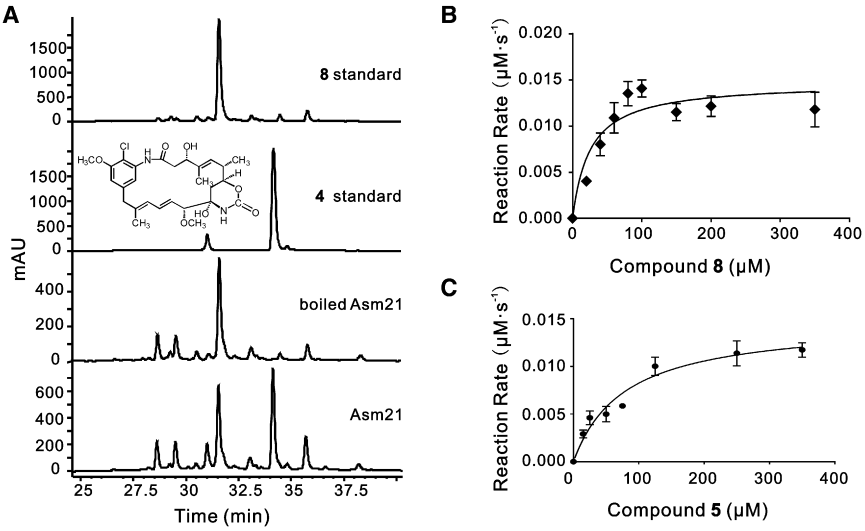

Figure 4. Kinetic Characterization of Asm21 with 8 or 5 as Substrate

(A) HPLC analysis of assays with **8** as substrate. Assay reactions were incubated at 30°C overnight with purified Asm21 or heat-denatured enzyme as negative control. See also Figure S2 and Figure S3.

(B) Initial velocity of carbamoylation of **8** as a function of the concentration of **8**.

(C) Initial velocity of carbamoylation of **5** as a function of the concentration of **5**. All results represent mean values of triplicate determinations and standard deviations.

Asm21 showed optimal activity at pH 8.5–9.0, and more than 70% of the maximal activity in the pH range of 8.0–11.0. The activity decreased dramatically at pH values lower than 7.5 (Figure S3B). Mg^{2+} was reported to be essential for the activity of a carbamoyltransferase (Brewer et al., 1980). Asm21 consistently showed the highest activity when supplied with 5–10 mM Mg^{2+}, considerable activity with 5 mM Mn^{2+} or Co^{2+}, but no activity with Ca^{2+}, Zn^{2+}, or Cu^{2+} (Figure S3C). Therefore, the subsequent kinetic studies on Asm21 were performed at 37°C and pH 8.5 with 10 mM $MgCl_2$ and 1 mM carbamoyl phosphate as described in the Supplemental Information. Besides **8**, Asm21 could also carbamoylate **5**, **6**, and **7** (Figures S2C and S2D).

The initial velocity was measured by varying the concentration of **8** at a fixed concentration of carbamoyl phosphate (1 mM). The product concentration was quantitated by Q-TOF MS. Compared to **5** with a K_m of 78.7 ± 18.8 μM, Asm21 shows higher affinity toward **8** with a K_m of 25.2 ± 8.7 μM. The k_{cat} values, 14.7 ± 1.1 s^{-1} and 14.7 ± 1.2 s^{-1} for **5** and **8**, respectively, and the catalytic efficiencies k_{cat}/K_m, 0.2 $\mu M^{-1}s^{-1}$ for **5** and 0.6 $\mu M^{-1}s^{-1}$ for **8**, also indicate that **8** is a preferred substrate for Asm21 (Figures 4B and 4C).This is in accordance with the intermediate accumulation pattern in solid cultures of BLQ16 (Figure 3A), albeit not in liquid cultures, which accumulate mainly **5** when Asm21 is inactivated (Spiteller et al., 2003).

Asm21 Catalyzes the Carbamoylation of C-4 Hydroxyl Group of the *N*-β-D-glucosyl Moiety of Ansamitocinoside P-3 (2)

The presumed substrate for carbamoylation, **2**, was prepared by in vitro glycosylation of PND-3 (**11**) with heterologously expressed soluble *N*-glycosyltransferase Asm25 (Zhao et al., 2008). Asm21 catalyzed the conversion of **2** into **3** as detected by Q-TOF MS (Figure 5A). Therefore Asm21 does have dual carbamoylation activity on both the polyketide backbone and the sugar moiety. Moreover, Asm21 has a K_m of 135.3 ± 38.4 μM for **2**, much higher than those for **5** or **8**, which indicates a favored binding mode placing the polyketide backbone rather than the glucosyl moiety in the reaction site of Asm21 (Figure 5B). However, it has a k_{cat} of 212.5 ± 24.0 s^{-1} for **2**, which is 14 times higher than those for **5** or **8**. The overall catalytic efficiency k_{cat}/K_m for **2** is 1.6 $\mu M^{-1}s^{-1}$ and thus higher than those for **5** (0.2 $\mu M^{-1}s^{-1}$) or **8** (0.6 $\mu M^{-1}s^{-1}$). Hence, the catalytic constants indicate that Asm21 displays a preference for carbamoylation of the glucosyl moiety over the polyketide backbone.

Dual Carbamoylations in Resting Cells

In order to demonstrate the dual action of Asm21 in *A. pretiosum,* **8** was fed to resting cells of HGF068 lacking the whole *asm* gene cluster and HGF051 that retains all the postmodification genes. The production of **3** ($[M + H]^+$ at m/z 826, $[M + Na]^+$ at m/z 848) was observed, and neither **8** nor the uncarbamoylated **2** was detectable in HGF051, indicating the high dual catalytic efficiency of Asm21. In addition, AP-3 (**1**), AP-2, AP-4, and quasi molecular ion peaks proposed to belong to ACGP-2 ($[M + Na]^+$ at m/z 834) and ACGP-4 ($[M + Na]^+$ at m/z 862) were also detected in the HGF051 extract. Meanwhile, no transformation of **8** was observed in the HGF068 extract (Figure 6 and Figures S4A–S4C).

DISCUSSION

The isolation of ansacarbamitocins (Snipes et al., 2007), carbamoylated ansamitocin derivative (Knobloch et al., 2011), and ACGP-3 (**3**) raised the question which gene and enzyme is responsible for the carbamoylation of the glucose hydroxyl group. The carbamoyltransferase-encoding gene *asm21* within the *asm* biosynthetic gene cluster was thought of as a potential candidate. Otherwise, there must be other genes in the genome to fulfill this function. The construction of numerous mutants of *A. pretiosum* ATCC 31565 in the previous work (Yu et al., 2002) allowed the convenient identification of the relevant functional carbamoyltransferase gene(s). HGF051 is a mutant with a truncated PKS *asmB* gene that retains the complete gene set for post-PKS modifications, including *asm21*. HGF068 is a mutant with a 200-kb deletion lacking the whole ansamitocin biosynthetic gene cluster. Because HGF051 could convert AGP-3 (**2**) into ACGP-3 (**3**) and HGF068 could not (Figure 2), the responsible carbamoyltransferase gene must be located within the 200-kb region. Bioinformatic analysis of the 90-kb available sequence of this region showed that *asm21* is the only carbamoyltransferase gene present. Asm21 had previously been

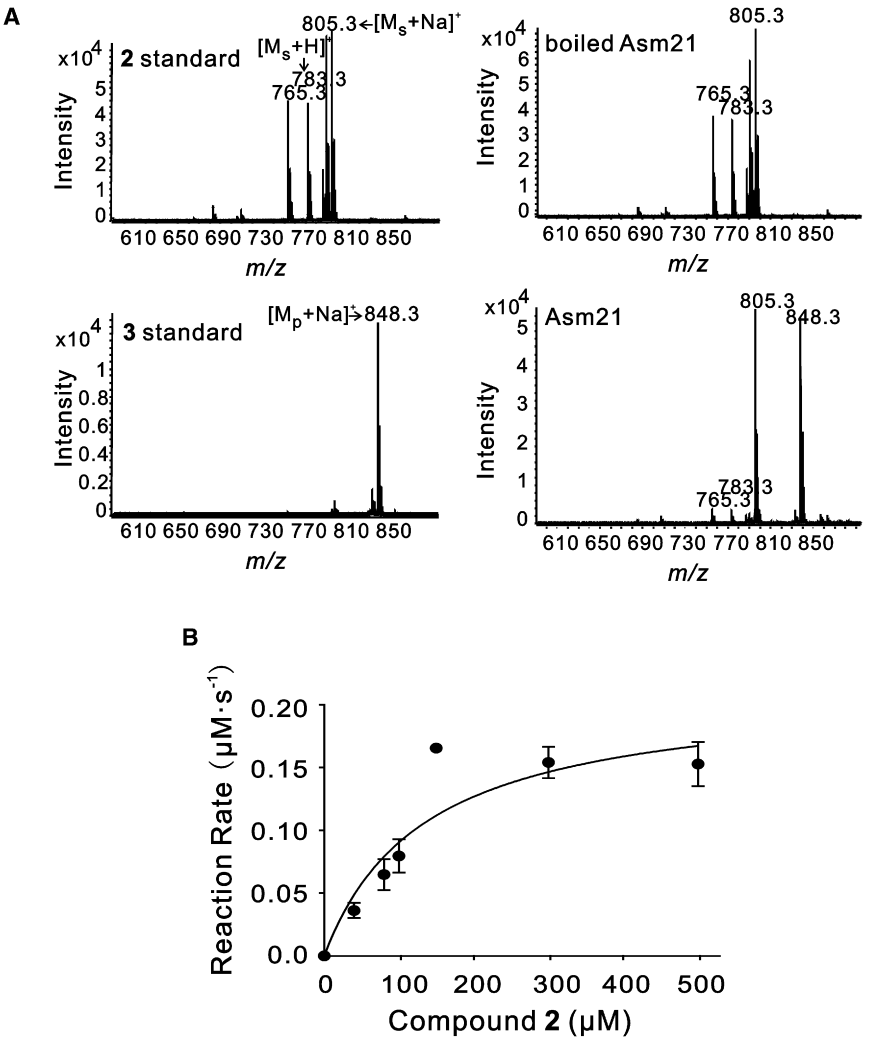

Figure 5. Kinetic Characterization of Asm21 with 2 as Substrate

(A) Q-TOF MS profiles of assays with **2** as substrate.

(B) Initial velocity of carbamoylation of **2** as a function of the concentration of **2**. M_s, Mw of **2**; M_p, Mw of **3**. All results represent mean values of triplicate determinations and standard deviations.

suggested to be responsible for the carbamoylation of the C-7 hydroxyl group of the ansamitocin backbone and the formation of the cyclic carbinolamide (Spiteller et al., 2003). Therefore the feeding experiments suggested that Asm21 has dual carbamoylation activity on both the polyketide backbone and the glucosyl moiety.

The *asm21* deletion mutant BLQ16 accumulated, in addition to the previously isolated **5** and **8** (Spiteller et al., 2003), equal amounts of two new compounds, **6** and **7**, which are diastereomers with opposite configurations at the newly generated stereocenter (Figure 3). Their formation probably does not represent a specific step in the ansamitocin biosynthetic pathway, but rather a pathway-unspecific biotransformation of the accumulated **8**. When **8** was fed to the resting cells of HGF068 (Figure 6), it underwent substantial biotransformation, during which the quasi molecular ion peaks corresponding to **6** and **7** ($[M + Na]^+$ at m/z 530, $[M + K]^+$ at m/z 546) could be found (Figure S4D). This suggests that the biotransformation from **8** to **6** or **7** is catalyzed by a general oxygenase encoded elsewhere in the genome. Nevertheless, **6** and **7** are still substrates for carbamoylation at C-7 by Asm21 (Figure S2D).

In the course of the complementation experiments with the *asm21*-disrupted mutant BLQ16, the previously proposed (Yu et al., 2002) 2007-bp ORF for *asm21* had to be revised to 2205-bp, extending the amino terminus of the protein by 66 amino acids. This N-terminal 66-aa segment of Asm21 was found to be required for carbamoyltransferase activity (Figure S1). However, because seven start codons can be found in this 198-bp region, more evidence is required to define the precise start codon for the translation of Asm21.

The cyclic carbinolamide group in ansamitocin is different from the linear carbamoyl groups in all other antibiotics. Its installation requires a second reaction after the carbamoylation at C-7, in which the amino group reacts with the C-9 carbonyl group, resulting in a six-membered ring and a free hydroxyl group. It is unclear whether this second step occurs spontaneously, as is chemically plausible, or is also enzymatically catalyzed. The *asm* biosynthetic gene cluster does not contain any likely candidate gene to encode such an enzyme. However, the fact that the C terminus of Asm21 is extended by 100 amino acids compared to other antibiotic carbamoyltransferases raised the question whether this region catalyzed the ring closure reaction. Complementation of the *asm21*-disrupted mutant BLQ16 with *asm21* truncated at the C terminus by 97 amino acids, however, failed to restore ansamitocin production (Figure S1), and did not lead to accumulation of compounds with a linear carbamoyl side chain. Thus, this region of Asm21 is essential for carbamoyltransferase activity, but probably not for ring closure. The latter might occur spontaneously either before or after release of the product of Asm21 from the enzyme.

In the post-PKS modification metabolic grid (Spiteller et al., 2003), carbamoylation catalyzed by Asm21 can occur both before and after *O*-methylation by Asm7, i.e., with **5** or **8** as substrate. Our kinetic data on Asm21 demonstrate that 8 is a 3-fold better substrate than **5**, suggesting that more of the flux through the grid proceeds via carbamoylation of **8**. Subsequently in the pathway, the glucosyl moiety is transferred to the macrolactam amide bond by the *N*-glycosyltransferase Asm25, and Asm21 acts again to transfer the carbamoyl group to the glucosyl moiety. Therefore, the tandem catalysis by

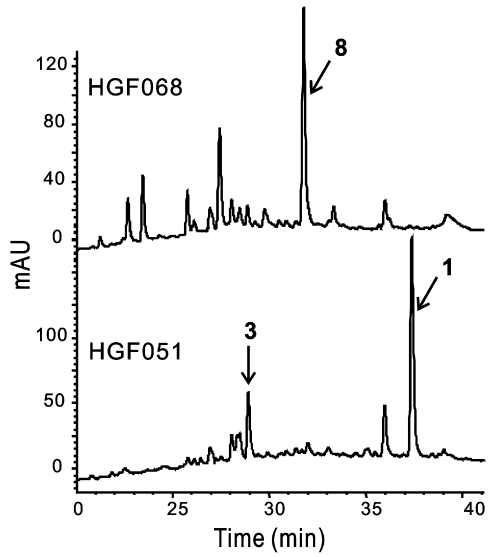

Figure 6. HPLC Analysis of the Conversion of 8 to 1 and 3 by Resting Cells of *A. pretiosum*
See also Figure S4.

Asm25 and Asm21 results in an extension of the ansamitocin biosynthetic pathway to carbamoylated ansamitocinosides (Figure 7).

As both our studies and the work of the Kirschning group show, Asm21 is an unusually promiscuous enzyme, which can transfer the carbamoyl group to the C-7 OH group in a wide range of structurally modified ansamitocins as well as to other OH groups in various ansamitocin derivatives and analogs. As shown by Knobloch et al. (2011), carbamoylation of the C-7 hydroxyl group by Asm21 will occur regardless of the substituents located in the aromatic western hemisphere. This is strongly supported by the carbamoylation of compound **6** or **7** by Asm21 in our study. Whether Asm21 is also responsible for the additional carbamoylations at the benzyl alcohol function (Knobloch et al., 2011) or other positions deserves further investigation in vitro. Deeper insights into the enzymatic mechanism of the multiple actions of Asm21 will require the X-ray structure determination of enzyme-substrate complexes to explain the impressive substrate flexibility of this enzyme.

SIGNIFICANCE

The 4″-*O*-carbamoyl ansamitocinoside (ACGP-3) isolated from *A. pretiosum* ATCC31565 is a novel ansamitocin derivative that is carbamoylated on both the polyketide backbone and the sugar moiety. The carbamoyltransferase Asm21 from the *asm* gene cluster was characterized by mutagenesis and complementation as well as heterologous expression and kinetic analysis. Remarkably, the enzyme catalyzes not only the C-7 carbamoylation of the macrolactam backbone, accepting a variety of ansamitocin structures as substrate, but also carbamoylation of the C-4 hydroxyl group of the *N*-glucosyl moiety in ansamitocinoside P-3. The dual action of Asm21 was validated in vivo and in vitro, representing the first full characterization of an antibiotic *O*-carbamoyltransferase with very high substrate flexibility. Thus, the ansamitocin biosynthetic pathway could be extended by cultivation on solid medium through the tandem catalysis of the *N*-glycosyltransferase Asm25 and the *O*-carbamoyltransferase Asm21. Due to its broad substrate range, Asm21 can be used to generate *O*-carbamoylated derivatives of many ansamycins as potential drug candidates.

EXPERIMENTAL PROCEDURES

Bacterial Strains, Plasmids, and Primers

For a complete list, see Table S1 in the Supplemental Information. *E. coli* strains DH10B (Invitrogen), ET12567/pUZ8002 and BLR(DE3)pLysE were used as hosts for cloning, *E. coli-Actinosynnema* bi-parental conjugation and protein overexpression, respectively. Plasmid pIJ2925 and pRSETb were used for construction. Plasmid pJTU1289 was used for the construction of the *asm21* mutant. The integrative vector pJTU824 was used for the complementation of the *asm21* mutant, and pRSETb was used for protein overexpression.

General Methods and Instrumentation

HPLC was performed on a Waters 2690 Separations Module and a 996 Photodiode Array Detector. Mass spectra were measured on an Agilent 1100 Series LC-MSD Trap. Preparative LC was carried out on a SHIMADZU LC-8A Preparative Liquid Chromatograph. Q-TOF MS analyses were performed on an Agilent 6530 Accurate-Mass Q-TOF LC-MS. NMR spectra were recorded on Bruker AM-400 or DRX-500 NMR spectrometers with TMS as internal standard. Silica GF254 for preparative plates and silica gel G precoated TLC plates were obtained from Qingdao Marine Chemical Factory, Qingdao, China. Sephadex LH-20 was purchased from Amersham Biosciences. C_{18} reversed phase silica gel, 200–300 mesh, used for column chromatography was obtained from Merck.

Actinosynnema pretiosum ssp. *aurantium* ATCC31565 and its derivatives were cultivated in liquid or solid yeast extract-malt extract-glucose (YMG) medium (0.4% yeast extract, 1% malt extract, and 0.4% glucose, pH 7.3) for ansamitocin production. Fermentations and extractions were carried out as described (Zhao et al., 2008). *E. coli* strains were cultivated at 37°C in Luria-Bertani medium or on Luria-Bertani agar plates. Total DNA was isolated from *Actinosynnema* as described by Kieser et al. (2000). Synthesis of oligonucleotide primers and DNA sequencing of PCR products were performed by Shanghai Sangon and Invitrogen. Extraction of DNA fragments from agarose gel slices was performed with the Gel Recovery Kit (Tiangen).

Isolation of Carbamoylated *N*-Ansamitocinoside (3, ACGP-3)

The solid culture agar of *A. pretiosum* was chopped up, diced, and extracted four times with the solvent mixture EtOAc/MeOH/AcOH (80:15:5, v/v/v), at room temperature. The residue of the extract (21 g) was subjected to MPLC on C_{18} reversed-phase silica gel (145 g), eluting with water containing increasing amounts of methanol, to produce four fractions (1–4). Fraction 2 (864 mg) was subjected to column chromatography on Sephadex LH-20 (130 g), eluting with MeOH, and then to MPLC on C_{18} reversed-phase silica gel (45 g), eluting with water containing increasing amounts of MeOH to obtain three fraction (2/1–2/3). Fraction 2/2 (240 mg) was dissolved in MeOH, and then subjected to thin-layer chromatography using preparative plates (Qingdao, GF254) with EtOAc/MeOH (5:1, v/v), containing 0.5 ml 25% ammonia in 100 ml, as the developing solvent. Densitometric analyses of the chromatograms were carried out with a ternary wave-length TLC scanner ZF-I at 254 nm (Ma et al., 2007). All the TLC plates, for analysis and preparation, were developed with the particular developing agent once or twice for optimal separation. All the compounds were subjected to column chromatography over Sephadex LH-20 (30 g) again eluting with acetone for purification. ^{1}H NMR (400 MHz), ^{13}C NMR (100 MHz), and 2-D NMR data are listed in Table S2. **3**, ESI *m/z* 848 $[M + Na]^{+}$; HR-ESI-MS m/z 848.2988 $[M + Na]^{+}$ (calculated for $C_{38}H_{52}N_3O_{15}ClNa$, 848.2984).

Resting Cell Preparation

A loopful of *A. pretiosum*, grown on YMG-agar, was used to inoculate 25 ml of YMG media in a 250 ml Erlenmeyer flask, which was incubated for 24 hr (30°C,

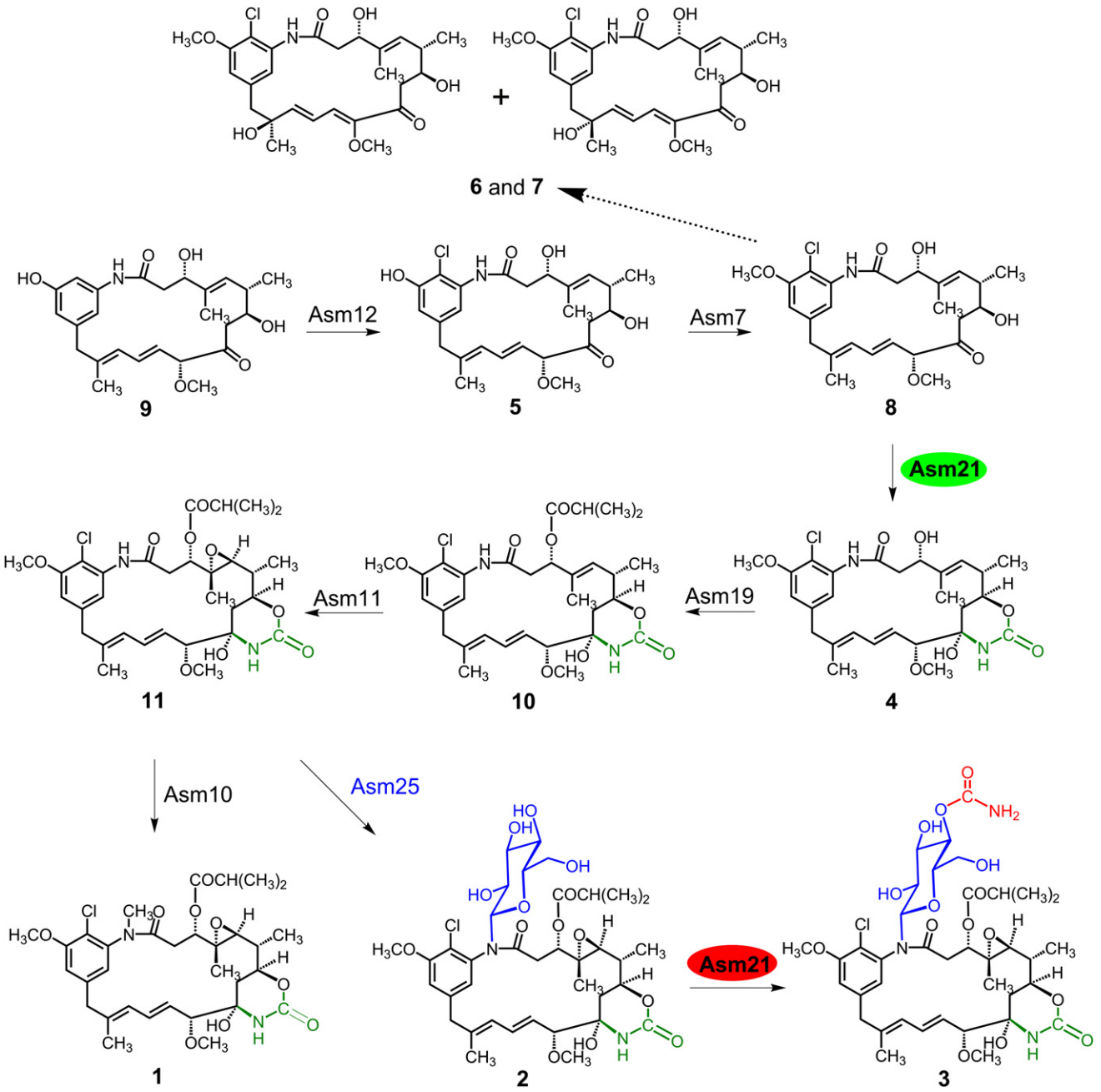

Figure 7. The Extended Post-PKS Modifications of Ansamitocin Biosynthesis
Dotted arrows indicate the biotransformation from **8** to **6** or **7** is catalyzed by a pathway-nonspecific oxygenase encoded elsewhere in the genome.

220 rpm). This seed culture was used to inoculate (1 ml each) multiple flasks of YMG (100 ml in a 500 ml Erlenmeyer flask). These batch cultures were incubated for 48 hr before being harvested by centrifugation (7,000 rpm, 12 min). The pellet was then washed three times with 0.2-volume equivalents of distilled water, and the cells suspended in 0.2-volume equivalents of water. The resting cell experiments were then initiated by adding the cell suspension (20 ml) in a 80 ml mixture of lactose (0.25 M, 20 ml), $MgCl_2$ (0.05 M, 10 ml), L-valine (0.10 M, 10 ml), Tris-HCl (0.1 M, pH 8.0, 10 ml), and double distilled water (30 ml). The cell density was now the same as prior to harvesting. The cultures were incubated for 72 hr and harvested by direct extraction with ethyl acetate (3-volume equivalent). The organic solvent was removed in vacuo, and the residue was resuspended in methanol for LC-MS analysis.

Inactivation of Carbamoyltransferase Gene *asm21*

The *asm21* gene was disrupted using the ReDirect technology (Gust et al., 2003). A 7509-bp SalI fragment carrying *asm21* was cloned from cosmid pDDc6 of the *A. pretiosum* ATCC 31565 genomic library into SalI-digested pIJ2925 to generate pJTU825. The same fragment with two additional BglII sites was then inserted into the BamHI site of pJTU1289 (He et al., 2010). The *asm21* gene from the resulting plasmid, pJTU826′, was replaced by the *aac(3)IV* and *oriT* cassette amplified from the pIJ773 disruption cassette with the primers asm21-del-F and asm21-del-R. The resulting pJTU827 was introduced into ATCC 31565 via *E. coli-Actinosynnema* biparental conjugation as described (Yu et al., 2002). Apramycin-resistant and thiostrepton-sensitive double crossover mutants were obtained after two rounds of

cultivation in liquid TSBY medium without apramycin or thiostrepton. The mutant was confirmed by asm21-det-F and asm21-det-R and named BLQ16.

Complementation of the *asm21* Mutant BLQ16 with PCR-Amplified *asm21* of Different Lengths

Different lengths of *asm21*, 1.7-kb, 2.0-kb, 2.2-kb, were amplified from pJTU825 using three pairs of primers: asm21-S-F/asm21-S-R, asm21-L-F/asm21-S-R, and asm21-L-F/asm21-R, respectively. Engineered BamHI and NdeI sites were contained in the forward primers, whereas an EcoRI site was located in the reverse primers. The amplified fragments were digested with BamHI and EcoRI and ligated into pRSETb, which had been treated with the same enzymes, to generate pJTU831, pJTU838, and pJTU3052, respectively. After sequencing, an internal 1661-bp BbsI fragment of pJTU838 and pJTU3052 were replaced by the same fragment from pJTU825 to ensure the complete sequence fidelity. An 1878-bp BamHI-BstXI fragment from pJTU3052 and an 2987-bp BamHI-BxtXI fragment were recovered and ligated together to generate pJTU3054 containing 1.9-kb *asm21* that could also be amplified using asm21-L-F/asm21-S-R. 1.7-kb, 1.9-kb, 2.0-kb, 2.2-kb DNA fragments containing *asm21* were cleaved from pJTU831, pJTU3054, pJTU838, and pJTU3052 by NdeI and EcoRI and cloned into pJTU824 (Wu et al., 2011b) to generate pJTU832, pJTU3055, pJTU839, and pJTU3053, respectively. All the plasmids were introduced into BLQ16 by conjugation. After incubation at 37°C for 12 hr, the plates were overlaid with 1 ml deionized water containing 1 mg nalidixic acid, 1 mg apramycin, and 250 μg thiostrepton. The thiostrepton-resistant exconjugants were confirmed by PCR using primers tsr-F/R for the thiostrepton resistance gene (*tsr*), and the fermentation broths were then analyzed by LC-MS.

Isolation and Structure Elucidation of Compounds from BLQ16

A seed culture of BLQ16 was prepared in liquid TSBY medium inoculated with fresh mycelia grown on YMG agar plates. After cultivation at 30°C and 220 rpm for 48 hr, 1 ml each of the culture was used to inoculate 70 ml YMG agar plates, 6 l in total. After fermentation at 30°C for 9 days, the agar was chopped into small pieces and extracted three times with EtOAc/MeOH/AcOH (80:15:5, v/v/v) to obtain a crude extract. The extract was subjected to macroporous resin XAD-16 (Amberlite), which was washed with 45% ethanol and eluted with 60% ethanol. The 60% ethanol eluate was concentrated, dissolved in 2 ml methanol and then injected in 200 μl samples onto a preparative SHIMADZU PRC-ODS column (55% methanol, flow rate: 4 ml/min, UV: 236 nm). The eluates were collected manually to give five fractions. Fractions B, C, D, and E were examined by LC-MS for the presence of the corresponding $[M + H]^+$ or $[M + Na]^+$ quasi molecular ion peak of the expected **5** or **8** and the two new peaks of **6** and **7**. All four fractions were subjected to a second HPLC purification under the same conditions. The purified compounds were analyzed by NMR and further used for the biochemical analysis. The NMR data are listed in Tables S3–S5.

Isolation of 4 and Preparation of AGP-3

N-Desmethyl-4,5-desepoxy-maytansinol (**4**) was isolated from the *asm19* mutant HGF052 as described previously (Wei et al., 2010). AGP-3 (**2**) was obtained by scale-up of the conversion of **11** (PND-3, isolated from the *asm10* mutant) and UDP-glucose catalyzed by purified soluble Asm25 expressed in a pET28a derivative vector (Wu et al., 2011a; Zhao et al., 2008).

LC-MS Analysis of Ansamitocins and Derivatives

LC-Electrospray ionization (ESI)-MS analysis was performed on an Agilent 1100 series instrument with an Agilent ZORBAX SB-C18 column (2.1 × 150 mm, 3.5 μm). The UV detection wavelengths were 254 nm and 236 nm. ESI mass spectrometry was carried out using chamber settings as follows: nebulizer pressure, 30 psi; drying gas flow, 10 l/min; drying gas temperature, 325°C. Samples were dissolved in methanol and analyzed at a flow rate of 0.1 ml/min with the following step gradient: 0–10 min 10% B, 10–20 min 55% B, 20–35 min 75% B, 35–45 min 90% B (solvent A, 99.8% water, 0.2% formic acid; solvent B, methanol). Analysis was carried out in positive ion mode with a mass range set to 400–900 Da.

Heterologous Expression and Purification of Recombinant His_6-Tagged Asm21

Transformants of *E. coli* BLR(DE3)pLysE harboring pJTU3052 were grown in LB medium supplemented with ampicillin (100 μg/ml), chloramphenicol (34 μg/ml), and tetracycline (12.5 μg/ml) overnight at 30°C, 220 rpm. Five ml of overnight culture was diluted with 150 ml fresh LBBS medium (10 g of tryptone, 5 g of yeast extract, 10 g of NaCl, 182.2 g of D-sorbitol, 0.309 g of betaine per liter) in a 500 ml flask (Eads et al., 1999). The culture was grown at 30°C for 12 hr, at 16°C for 12 hr to OD_{600} = 0.8–1.0, and induced with 0.1 mM IPTG at 16°C for another 24 hr. After induction, the *E. coli* cells from 1 l culture were centrifuged at 7,000 rpm for 30 min and the pellet was suspended in 50 ml buffer A (20 mM Tris-HCl, pH 8.0, 300 mM NaCl) supplemented with an EDTA-free Protease Inhibitor Cocktail Tablet (Roche). After disruption by three passes through a French Press (Thermo), the cell debris was removed by centrifugation (12,500 rpm, 40 min). The protein was purified from the soluble cell extract by metal affinity chromatography using His-Bind Resin (Merck-Novagen) according to the manufacturer's instructions. The fractions were eluted by buffer A containing 100 mM, 150 mM, 200 mM, or 1 M imidazole, up to 100 ml in total, and concentrated to 1 ml in buffer A in a 50-kD Amicon Ultra-15 Centrifugal Filter (Millipore). Protein concentrations were determined by the Bradford method (Tiangen, PA102) with bovine serum albumin (BSA) as standard. SDS-PAGE was carried out according to the method of Laemmli, and protein bands were stained with Coomassie Brilliant Blue R250.

Enzymatic Assays and Identification of the Products

The carbamoyltransferase assay mixture contained 50 mM Tris-HCl (pH 8.0), 200 mM NaCl, 5 mM $MgSO_4$, 2 mM DTT, 1% BSA, 5% DMSO, 2 mM ATP, 1 mM carbamoyl phosphate disodium, 0.5 mM **8**, and purified Asm21 (1 μM) in a final volume of 200 μl. The reactions were carried out at 30°C overnight and terminated by addition of 200 μl ethyl acetate. The assay products were extracted twice with ethyl acetate. After evaporation of the organic solvent, the residues were dissolved in methanol and analyzed by LC-MS as described above.

Quantification and Kinetic Analysis

Enzymatic assays with **8** were carried out in a total volume of 100 μl as above, containing typically 0.3–3.2 μM of Asm21. The reactions were carried for a suitable time interval during which the rate of product formation was linear with time (10–60 min) and quenched with 50 μl *n*-butanol. After centrifugation at 12,000 rpm for 10 min, 10 μl aliquots of supernatant were analyzed by analytical HPLC (Waters) with an XTerraTM RP18 column (Waters, 5 μm, 3.9 × 150 mm; 55% methanol, 0.2 ml/min). The UV absorption of authentic **4** was integrated automatically by software Millennium32 (Waters) based on a standard curve. The concentration of **4** in the reaction mixture was then calculated.

Kinetic parameters of **2**, **5**, and **8** were determined with constant concentration of carbamoyl phosphate (1 mM). The concentration of substrates varied between 10 and 500 μM. The reactions were carried out at optimal conditions with an Asm21 concentration of 1 μM and terminated by addition of 100 μl *n*-butanol. After centrifuged at 12,000 rpm for 10 min, 20 μl aliquots of the supernatants were diluted to 1 ml with methanol and then quantified by Q-TOF MS. The expected quasi molecular ion was extracted from the total ion chromatogram (TIC), and calibrated by the Agilent MassHunter Qualitative Analysis Software. The calibration curve was constructed based on peak areas of each carbamoylated product at m/z 848, 543, and 557 $[M + Na]^+$ for **2**, **5**, and **8**, respectively. The initial concentration of the product was then calculated according to the calibration curves. All the experiments were performed in triplicate. K_m and k_{cat} values were determined with the GraphPad Prism 5 software (Neumann et al., 1996).

SUPPLEMENTAL INFORMATION

Supplemental Information includes four figures, and five tables and can be found with this article online at doi:10.1016/j.chembiol.2011.11.007.

ACKNOWLEDGMENTS

The authors are grateful to Prof. Heinz G. Floss and Yuemao Shen for critical discussions and help in manuscript preparation. This work received financial

support from the National Natural Science Foundation of China, the Ministry of Science and Technology (973 and 863 Programs), the Ministry of Education, and the Shanghai Municipality.

Received: October 4, 2011
Revised: October 29, 2011
Accepted: November 7, 2011
Published: December 22, 2011

REFERENCES

Brewer, S.J., Taylor, P.M., and Turner, M.K. (1980). An adenosine triphosphate-dependent carbamoylphosphate—3-hydroxymethylcephem O-carbamoyltransferase from *Streptomyces clavuligerus*. Biochem. J. *185*, 555–564.

Cassady, J.M., Chan, K.K., Floss, H.G., and Leistner, E. (2004). Recent developments in the maytansinoid antitumor agents. Chem. Pharm. Bull. (Tokyo) *52*, 1–26.

Chari, R.V. (2008). Targeted cancer therapy: conferring specificity to cytotoxic drugs. Acc. Chem. Res. *41*, 98–107.

Eads, J.C., Beeby, M., Scapin, G., Yu, T.W., and Floss, H.G. (1999). Crystal structure of 3-amino-5-hydroxybenzoic acid (AHBA) synthase. Biochemistry *38*, 9840–9849.

Flatman, R.H., Eustaquio, A., Li, S.M., Heide, L., and Maxwell, A. (2006). Structure-activity relationships of aminocoumarin-type gyrase and topoisomerase IV inhibitors obtained by combinatorial biosynthesis. Antimicrob. Agents Chemother. *50*, 1136–1142.

Floss, H.G., Yu, T.W., and Arakawa, K. (2011). The biosynthesis of 3-amino-5-hydroxybenzoic acid (AHBA), the precursor of mC7N units in ansamycin and mitomycin antibiotics: a review. J. Antibiot. *64*, 35–44.

Freel Meyers, C.L., Oberthür, M., Xu, H., Heide, L., Kahne, D., and Walsh, C.T. (2004). Characterization of NovP and NovN: completion of novobiocin biosynthesis by sequential tailoring of the noviosyl ring. Angew. Chem. Int. Ed. Engl. *43*, 67–70.

Gellert, M., O'Dea, M.H., Itoh, T., and Tomizawa, J. (1976). Novobiocin and coumermycin inhibit DNA supercoiling catalyzed by DNA gyrase. Proc. Natl. Acad. Sci. USA *73*, 4474–4478.

Gust, B., Challis, G.L., Fowler, K., Kieser, T., and Chater, K.F. (2003). PCR-targeted *Streptomyces* gene replacement identifies a protein domain needed for biosynthesis of the sesquiterpene soil odor geosmin. Proc. Natl. Acad. Sci. USA *100*, 1541–1546.

Haydock, S.F., Appleyard, A.N., Mironenko, T., Lester, J., Scott, N., and Leadlay, P.F. (2005). Organization of the biosynthetic gene cluster for the macrolide concanamycin A in *Streptomyces neyagawaensis* ATCC 27449. Microbiology *151*, 3161–3169.

He, Y., Wang, Z., Bai, L., Liang, J., Zhou, X., and Deng, Z. (2010). Two pHZ1358-derivative vectors for efficient gene knockout in *streptomyces*. J. Microbiol. Biotechnol. *20*, 678–682.

Higashide, E., Asai, M., Ootsu, K., Tanida, S., Kozai, Y., Hasegawa, T., Kishi, T., Sugino, Y., and Yoneda, M. (1977). Ansamitocin, a group of novel maytansinoid antibiotics with antitumour properties from *Nocardia*. Nature *270*, 721–722.

Hooper, D.C., Wolfson, J.S., McHugh, G.L., Winters, M.B., and Swartz, M.N. (1982). Effects of novobiocin, coumermycin A1, clorobiocin, and their analogs on *Escherichia coli* DNA gyrase and bacterial growth. Antimicrob. Agents Chemother. *22*, 662–671.

Ishikawa, J., and Hotta, K. (1999). FramePlot: a new implementation of the frame analysis for predicting protein-coding regions in bacterial DNA with a high G + C content. FEMS Microbiol. Lett. *174*, 251–253.

Kieser, T., Bibb, M.J., Buttner, M.J., Charter, K.F., and Hopwood, D.A., eds. (2000). Practical *Streptomyces* Genetics (Norwich, United Kingdom: The John Innes Foundation).

Kinashi, H., Someno, K., and Sakaguchi, K. (1984). Isolation and characterization of concanamycins A, B and C. J. Antibiot. *37*, 1333–1343.

Knobloch, T., Harmrolfs, K., Taft, F., Thomaszewski, B., Sasse, F., and Kirschning, A. (2011). Mutational biosynthesis of ansamitocin antibiotics: A diversity-oriented approach to exploit biosynthetic flexibility. ChemBioChem *12*, 540–547.

Kupchan, S.M., Sneden, A.T., Branfman, A.R., Howie, G.A., Rebhun, L.I., McIvor, W.E., Wang, R.W., and Schnaitman, T.C. (1978). Structural requirements for antileukemic activity among the naturally occurring and semisynthetic maytansinoids. J. Med. Chem. *21*, 31–37.

Lewis, R.J., Singh, O.M., Smith, C.V., Skarzynski, T., Maxwell, A., Wonacott, A.J., and Wigley, D.B. (1996). The nature of inhibition of DNA gyrase by the coumarins and the cyclothialidines revealed by X-ray crystallography. EMBO J. *15*, 1412–1420.

Lu, C., Bai, L., and Shen, Y. (2004). A novel amide *N*-glycoside of ansamitocins from *Actinosynnema pretiosum*. J. Antibiot. *57*, 348–350.

Ma, J., Zhao, P.J., and Shen, Y.M. (2007). New amide *N*-glycosides of ansamitocins identified from *Actinosynnema pretiosum*. Arch. Pharm. Res. *30*, 670–673.

Miller, T.W., Goegelman, R.T., Weston, R.G., Putter, I., and Wolf, F.J. (1972). Cephamycins, a new family of beta-lactam antibiotics. II. Isolation and chemical characterization. Antimicrob. Agents Chemother. *2*, 132–135.

Nagarajan, R., Boeck, L.D., Gorman, M., Hamill, R.L., Higgens, C.E., Hoehn, M.M., Stark, W.M., and Whitney, J.G. (1971). Beta-lactam antibiotics from *Streptomyces*. J. Am. Chem. Soc. *93*, 2308–2310.

Neumann, A., Wohlfarth, G., and Diekert, G. (1996). Purification and characterization of tetrachloroethene reductive dehalogenase from *Dehalospirillum multivorans*. J. Biol. Chem. *271*, 16515–16519.

Snipes, C.E., Duebelbeis, D.O., Olson, M., Hahn, D.R., Dent, W.H., 3rd, Gilbert, J.R., Werk, T.L., Davis, G.E., Lee-Lu, R., and Graupner, P.R. (2007). The ansacarbamitocins: polar ansamitocin derivatives. J. Nat. Prod. *70*, 1578–1581.

Spiteller, P., Bai, L., Shang, G., Carroll, B.J., Yu, T.W., and Floss, H.G. (2003). The post-polyketide synthase modification steps in the biosynthesis of the antitumor agent ansamitocin by *Actinosynnema pretiosum*. J. Am. Chem. Soc. *125*, 14236–14237.

Steffensky, M., Mühlenweg, A., Wang, Z.X., Li, S.M., and Heide, L. (2000). Identification of the novobiocin biosynthetic gene cluster of *Streptomyces spheroides* NCIB 11891. Antimicrob. Agents Chemother. *44*, 1214–1222.

Wei, G.Z., Bai, L.Q., Yang, T., Ma, J., Zeng, Y., Shen, Y.M., and Zhao, P.J. (2010). A new antitumour ansamitocin from *Actinosynnema pretiosum*. Nat. Prod. Res. *24*, 1146–1150.

Wu, Y., Kang, Q., Shang, G., Spiteller, P., Carroll, B., Yu, T.W., Su, W., Bai, L., and Floss, H.G. (2011a). *N*-methylation of the amide bond by methyltransferase *asm10* in ansamitocin biosynthesis. ChemBioChem *12*, 1759–1766.

Wu, Y., Kang, Q., Shen, Y., Su, W., and Bai, L. (2011b). Cloning and functional analysis of the naphthomycin biosynthetic gene cluster in *Streptomyces* sp. *CS*. Mol. Biosyst. *7*, 2459–2469.

Xu, H., Heide, L., and Li, S.M. (2004). New aminocoumarin antibiotics formed by a combined mutational and chemoenzymatic approach utilizing the carbamoyltransferase NovN. Chem. Biol. *11*, 655–662.

Yu, T.W., Bai, L., Clade, D., Hoffmann, D., Toelzer, S., Trinh, K.Q., Xu, J., Moss, S.J., Leistner, E., and Floss, H.G. (2002). The biosynthetic gene cluster of the maytansinoid antitumor agent ansamitocin from *Actinosynnema pretiosum*. Proc. Natl. Acad. Sci. USA *99*, 7968–7973.

Zhao, P., Bai, L., Ma, J., Zeng, Y., Li, L., Zhang, Y., Lu, C., Dai, H., Wu, Z., Li, Y., et al. (2008). Amide *N*-glycosylation by Asm25, an *N*-glycosyltransferase of ansamitocins. Chem. Biol. *15*, 863–874.

